# Electronic structure and interfacial geometry of epitaxial two-dimensional Er silicide on Si(111)

L. Stauffer, A. Mharchi, C. Pirri, P. Wetzel, D. Bolmont, and G. Gewinner
*Laboratoire de Physique et de Spectroscopie Electronique, Faculté des Sciences et Techniques, 4 rue des Frères Lumière, 68093 Mulhouse CEDEX, France*

C. Minot
*Laboratoire de Chimie Organique Théorique, Université Pierre et Marie Curie, 4 Place Jussieu, 75252 Paris CEDEX 05, France*

(Received 9 October 1992)

The two-dimensional band structure of a single epitaxial $ErSi_2$ layer on Si(111) is calculated by means of the crystalline extension of the extended Hückel method for various atomic structures and tested against experimental bands determined by angle-resolved photoemission. In particular, adopting for the silicide layer the structure proposed in previous work, i.e., a hexagonal Er monolayer underneath a buckled Si top layer, various possible interfacial geometries are investigated, namely with the Er in top, substitutional, $T_4$, and $H_3$ sites of the Si(111) substrate and for the two possible orientations of the latter with respect to the buckled Si top layer. With the exception of the substitutional site, all models show two characteristic bands near the Fermi level that are essentially full and empty, respectively, as observed experimentally. Yet, the topology of these bands is correctly reproduced for only two interfacial geometries, namely Er in $H_3$ ($T_4$) sites with the buckled Si top layer having an orientation identical (opposite) to the substrate Si double layers. For both models the overall agreement between calculated and experimental bands is quite satisfactory. The prominent almost-filled band observed experimentally in the 0–1.7-eV binding-energy range mainly derives from the dangling bonds of the buckled Si top layer, but shows a strong hybridization with Er $5d$ states near the center of the surface Brillouin zone.

## I. INTRODUCTION

In recent years, much effort has been devoted to the growth of thin epitaxial silicide films with a good structural perfection on Si(111). Besides the extensively studied transition-metal disilicides $CoSi_2$ and $NiSi_2$,[1,2] rare-earth silicides exhibit some intriguing and promising features. In particular, $ErSi_{2-x}$ appears to be attractive for both the Si-based technology in microelectronics and fundamental studies on physical properties of ultrathin films and two-dimensional (2D) systems. Indeed, on the one hand, this silicide is characterized by a very low Schottky barrier to $n$-type Si[3] combined with a good electrical conductivity.[4] On the other hand, $ErSi_{2-x}$ grows epitaxially on Si(111) by either codeposition and annealing or solid-phase epitaxy.[5,6] Recently,[7] we have shown that a uniform well-ordered single layer of silicide with $ErSi_2$ stoichiometry and $p(1\times1)$ symmetry can be easily prepared by depositing one Er monolayer (ML) and annealing at 400 °C. Angle-resolved photoemission[8] confirms the 2D character of this layer which is a unique example of epitaxial surface silicide on Si(111). Bulk $ErSi_{2-x}$ ($x\simeq0.30$) crystallizes in a hexagonal phase with a defected structure of the $AlB_2$ type. The atomic arrangement consists of two kinds of basal planes, which are either Si in a graphitelike array or Er in a hexagonal array, piled up alternatively along the [0001] direction. The presence of an ordered array of Si vacancies accounts for the specific 1/1.7 stoichiometry and gives rise to a $\sqrt{3}\times\sqrt{3}\ R\ 30°$ superstructure observed in low-energy electron diffraction (LEED). The driving force for the formation of vacancies is apparently the compressive strain present in the graphitelike Si(0001) planes, which would result in Si-Si interatomic distances of 2.18 Å, as opposed to 2.35 Å in bulk Si. However, there is evidence that the surface termination of $ErSi_{1.7}$ films has $ErSi_2$ stoichiometry with a reconstructed Si top layer, which can be viewed as a distorted version of a graphitelike (honeycomb) Si plane where one out of two Si is displaced outwards so that a buckled Si top layer, similar to a Si(111) double layer in bulk Si, is formed at the surface.[7] Photoelectron and Auger electron-diffraction measurements, along with single-scattering simulations,[7–9] demonstrate that the single-layer surface silicide adopts the same structure, i.e., a hexagonal Er monolayer underneath a buckled Si top layer, as depicted in Fig. 1. It is also found that the space group of the surface silicide is $p3m1$ with an orientation of buckled Si top layer opposite to the substrate Si(111) double layers.[9] Yet, little is known about the interfacial geometry of the surface silicide, i.e., how the $ErSi_2$ layer binds to the Si(111) substrate.

It is clear that much can be learned about the growth and properties of thicker, technologically more interesting layers from a detailed understanding of the atomic and electronic structure of 2D $ErSi_2$. The past two decades have shown that the determination of the surface atomic structure and the study of surface electronic bands are clearly related problems. In this respect, a fairly detailed band structure of the surface silicide could be inferred from angle-resolved photoemission spectroscopy (ARPES), and a preliminary account of the results was

 ©1993 The American Physical Society

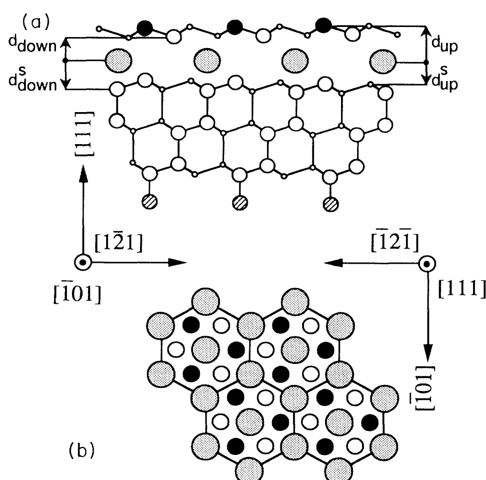


FIG. 1. Typical structure of the slabs used in the band calculations: (a) atomic structure projected along the [$\bar{1}$01] direction and (b) top view of the same structure. Large solid circles refer to Er species and small circles to Si atoms. Small solid circles indicate the topmost Si species displaced outwards with respect to their positions in bulk $ErSi_{1.7}$. The Si substrate is modeled by an $n$-atomic-double-layer slab with backface dangling bonds saturated by one-orbital atoms, shown as hatched circles. The meaning of the structural parameter $d_{up}$, $d_{down}$, $d^s_{up}$, and $d^s_{down}$ is indicated and the interfacial geometry shown corresponds to $T_4$-$B$ as defined in the main text.

presented in Ref. 8. It is the purpose of the present paper to give a more complete picture of the experimental 2D band dispersions along symmetry lines in the surface Brillouin zone (SBZ) and to compare them with surface bands calculated by means of the crystalline extension of the extended Hückel theory (EHT). This is an approximate semiempirical method originating from quantum chemistry[10–13] and similar to the tight-binding technique of physicists. In a first approximation, it appears to be a useful method for the study of rather complex surface compounds, surface structures, and thin films. In particular, it readily provides a first guide to the interpretation of the spectroscopic data. For instance, in the present case, where the interfacial geometry is not known, it allows us to test many plausible atomic structures without the heavy computations involved in *ab initio* methods. When the model of Ref. 7 is adopted, a quite satisfactory simulation of the experimental bands is obtained for two interfacial geometries, namely with Er in either $H_3$ or $T_4$ sites of the substrate and the buckled Si top layer having an orientation either identical or opposite, respectively, to the substrate Si double layers. The calculations clearly support the structural model proposed for the single silicide layer in Ref. 7, and favor two particular interfacial geometries. With the experimental finding[9] that the top Si double layer is rotated by 180° with respect to the substrate, one is then left with the $T_4$ site as the most likely atomic configuration at the interface. Moreover, the transparency of the EHT method allows us to obtain valuable information on the orbital origin of the various bands observed experimentally. This contributes to a better understanding of the ill-known electronic structure and outstanding properties of rare-earth silicide films.

## II. EXPERIMENTAL BAND STRUCTURE

The measurements were performed in an ultrahigh vacuum (UHV) chamber ($P \sim 10^{-10}$ Torr) equipped with LEED and high-resolution ARPES. The photoemission spectra were measured with He I ($\hbar\omega = 21.2$ eV), He II (40.8 eV), and Ne I (16.8 eV) excitations. The half-acceptance angle and energy resolution of the hemispherical analyzer were set to 1° and $\sim 50$ meV (He I), respectively. Er was evaporated onto clean Si(111) 7×7 from a homemade source at a rate of about 1 ML/min and a base pressure below $2.10^{-10}$ Torr. The ML scale is referred to the surface density of Si on ideal Si(111) surface. The evaporation rate was carefully calibrated by means of a quartz-crystal microbalance as well as core-level photoemission.

According to the recipe established in a previous work,[7] the Er surface silicide film was prepared by annealing at 400 °C of 1 ML Er deposited onto clean Si(111) at RT. The layer formed in this way is characterized by a very sharp $p\,(1\times1)$ LEED pattern that exhibits a pronounced threefold symmetry. This is the silicide layer studied in this work. Higher amounts of Er result in a $\sqrt{3}\times\sqrt{3}$ $R$ 30° pattern, which indicates the presence of bulk $ErSi_{1.7}$. On the other hand, for Er coverages below 1 ML, the same surface compound as for 1 ML is obtained but in the form of 2D islands, which do not cover the whole surface.[7] The Er surface silicide shows a very sharp and strongly dispersive surface features in the angle-resolved spectra, suggesting a high degree of crystallinity and indicating the need of high-resolution experiments.

Since typical spectra and details of their interpretation are shown and discussed in Ref. 8, we concentrate here on the final picture of 2D band dispersions inferred from the rough data. Figure 2 shows the result of a large body of experiments, using various collection geometries and photon energies. The data are folded back into the first SBZ along the three symmetry lines, namely $\bar{\Gamma}\bar{M}$, $\bar{\Gamma}\bar{K}$, and $\bar{K}\,\bar{M}$. The $k_{\parallel}(E)$ dispersions are obtained in the usual way by measuring the binding energy $E$ of the spectral peaks and calculating $k_{\parallel}$ with

$$k_{\parallel} = 0.512(\hbar\omega - E - \phi)^{1/2}\sin\theta ,$$

where $k_{\parallel}$ is the component of crystal momentum parallel to the surface, $\hbar\omega$ is the photon energy, $\theta$ is the polar angle of emission referred to the surface normal, and $\phi = 4.64$ eV is the measured work function. Many spectral features seen in the 0–5-eV binding-energy (BE) range correspond to bands that clearly display a 2D character in the $p\,(1\times1)$ SBZ. The relevant peaks, in particular in the 0–3 eV BE range, can generally be followed over the whole Brillouin zone. At higher binding energies, spectral structures, directly related to bulk Si substrate emission, can also be identified. For the sake of clarity, not all experimental peaks are represented in Fig. 2, where an effort has been made to plot mainly those data with a marked 2D character, i.e., showing periodicity in the extended zone scheme and little or no depen-

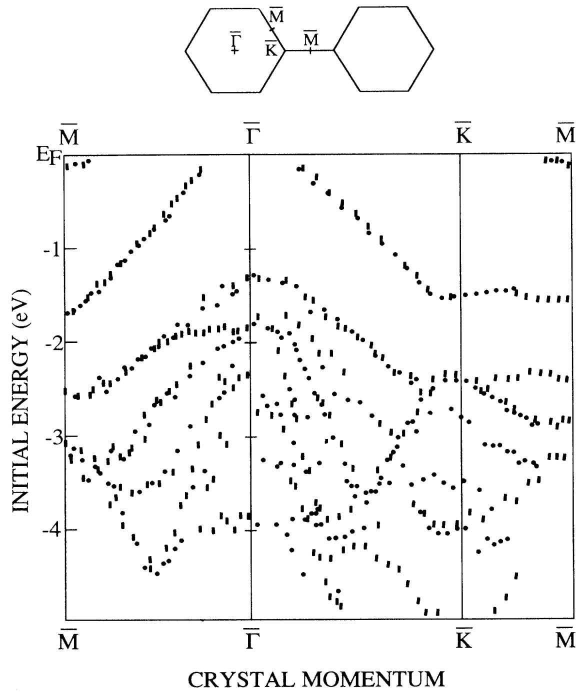


FIG. 2. Experimental band dispersions along $\bar{\Gamma}\bar{M}$, $\bar{\Gamma}\bar{K}$, and $\bar{K}\bar{M}$ for 1-ML Er on Si(111) annealed at 400 °C. The data were collected with He I (■) and Ne I (●) photon energies. The inset shows the $p(1\times1)$ surface Brillouin zone.

dence on photon energy. Thus most data points either reflect true surface states in the gap of the surface projected Si bulk band structure, or strong surface resonances elsewhere. The most prominent surface bands visible in the spectra correspond to a nearly filled one that crosses the Fermi level near $\bar{\Gamma}$ and a nearly empty one only visible around $\bar{M}$. At higher binding energies, several bands with strong antibonding character at $\bar{\Gamma}$ can be identified. It can be seen in Fig. 2 that the surface silicide is a semimetal with small hole and electron pockets at $\bar{\Gamma}$ and $\bar{M}$, respectively. These pockets are found to be almost circular in shape, and the ratio of their diameters is close to the value of $\sqrt{3}$ expected from geometry of the SBZ and charge conservation.[8]

## III. CALCULATED BAND STRUCTURES

### A. Computational method

The calculations use the crystalline extension of the EHT.[10–13] This method relies on an expansion of the electron wave functions into linear combinations of atomic orbitals in the form of Bloch sums. In the present case, the 2D periodic system is a slab defined by a unit cell and two translation vectors. The set of valence orbitals $|i\rangle$ per unit cell includes $3s,3p$ for Si and $5d,6s,6p$ for Er. The corelike Er $4f$ electrons are ignored, and the Er configuration is assumed to be $5d^16s^24f^{11}$ with three valence electrons. In contrast with the usual tight-binding approximation, the overlap between neighboring atomic orbitals is not neglected, and the energy levels $E(k_\parallel)$ are the solutions to the equation

$$\mathrm{Det}|H(k_\parallel)-ES(k_\parallel)|=0\ .$$

The overlap integrals in $S_{ij}(k_\parallel)$ are calculated from their definition using atomic orbitals of the Slater type. The intra-atomic matrix elements $H_{ii}$ involved in the $H_{ii}(k_\parallel)$ Bloch sums are derived from atomic energy levels (referred to the vacuum level), and the nondiagonal elements $H_{ij}$ are evaluated from the $H_{ii}$ and overlap integrals $S_{ij}$ using a formula of the Wolfsberg-Helmholtz-type.[14] The Slater exponents and atomic energy levels used are summarized in Table I. The Fermi energy $E_F$ is determined from a calculation of the $E(k_\parallel)$ for a uniform grid of $k_\parallel$ points (typically ~200 points) in the irreducible part of the SBZ. The slabs used in the calculations include the single silicide layer and a number of Si(111) double layers from substrate. A typical structure is shown in Fig. 1. The dangling bonds left at the backface of the slab are saturated by one-orbital atoms (denoted BFA), so that the limited number of substrate layers provides a good simulation of the semi-infinite Si(111) crystal. Five Si double layers are used in the calculations presented here. Test calculations show that adding further layers does not result in an appreciable change of the silicide-related bands. A series of possible atomic structures have been tested. Most calculations assume the structure of Ref. 7 for the silicide layer. As can be seen in Fig. 1, it consists of hexagonal Er monolayer and a buckled Si top layer characterized by interlayer distances $d_{\mathrm{up}}$ and $d_{\mathrm{down}}$. There are several ways to bind the silicide layer to the Si(111) substrate, all consistent with the $p3m1$ symmetry group of the system. Let us first assume an undistorted Si(111) substrate made of Si double layers with bulk geometry. The Er can be located either in top (T) sites, i.e., on top of Si atoms of the first Si(111) plane of the substrate, or in threefold hollow sites. There are two kinds of sites of the latter type. In the so-called $T_4$ site the Er is above the second-layer Si atom, and in the $H_3$ site it is above the hollow of the first Si double layer. For each of these different registries with respect to the Si(111) substrate, the silicide Si double layer may be oriented in the same way as the substrate double layers (orientation $A$) or rotated by 180° around surface normal (orientation $B$). Thus, one is left with six alternative simple interfacial geometries, characterized by three parameters, namely $d_{\mathrm{up}}$, $d_{\mathrm{down}}$, and $d^s_{\mathrm{up}}$, the distance of the Er layer to the first Si(111) plane of the substrate. Relevant atomic geometries are depicted in Fig. 3. According to the site and orientation involved, we call them $T$-$A$, $T$-$B$, $H_3$-$A$, $H_3$-$B$, $T_4$-$A$, and $T_4$-$B$, respectively. More sophistication may be introduced into these models by allowing

TABLE I. Parameters of the calculations.

| Orbital | $H_{ii}$ (eV) | Slater exponent |
|---|---|---|
| Er 6s | −4.882 | 1.396 |
| Er 6p | −4.882 | 1.396 |
| Er 5d | −6.917 | 2.199 |
| Si 3s | −17.30 | 1.450 |
| Si 3p | −9.20 | 1.450 |
| BFA 3s | −11.20 | 1.450 |

for a relaxation of the first Si layers of the substrate. If only the first double layer is allowed to relax, one needs an additional parameter $d^s_{\rm down}$, the distance of the Er layer to the second Si(111) layer of the substrate, to describe the structure. In these models, the atomic basis of the 2D unit cell contains one BFA, 12 Si atoms, and one Er atom, for a total of 52 valence electrons.

The above models for the surface silicide all strongly resemble the bulk $ErSi_2$ geometry, since the Er layer is sandwiched between two buckled, respectively defected, graphitelike Si layers. In this respect, we have also tested two more models called *S-A* and *S-B* that more strongly deviate from bulklike geometry. In these configurations the Er occupies substitutional sites, i.e., replaces the Si in the first Si(111) plane of the substrate. This model is characterized by $d_{\rm up}$, $d_{\rm down}$, and $d^s_{\rm down}$ and an atomic basis of the 2D unit cell made of one BFA, 11 Si, and one Er. This geometry is also depicted in Fig. 3 for the two orientations of the Si top double layer.

### B. Results and comparison with experiments

In a first attempt to reproduce and understand the origin of the experimental bands, we performed a series of calculations with $d_{\rm down}=2.0$ Å, $d_{\rm up}=2.7$ Å, and the following parameters: for the $H_3$ and $T_4$ sites, $d^s_{\rm up}=2.0$ Å, for $T$ sites, $d^s_{\rm up}=3.0$ Å, and for $S$ sites, $d^s_{\rm up}=2.0$ Å. This choice of parameter values is expected to be a good starting point since it ensures an Er-Si bond length very close to the bulk value of 3.02 Å observed in bulk $ErSi_{1.7}$, and it is consistent with the buckling of the Si top layer of 0.7–0.8 Å estimated in Ref. 7. The calculated bands for the various interfacial atomic structures are presented in Figs. 4–7. At this stage we concentrate on those bands located near the Fermi level $E_F$ at binding energies lower than ~2 eV, where the experiment shows the most clear-cut and unambiguous picture. Indeed, as expected, the calculations indicate that the electron states at higher binding energies are not localized in the silicide layer, but connect to bulklike states related to the Si layers that simulate the substrate. For all interfacial geometries, save *S-A* and *S-B*, one observes two bands near $E_F$. The upper band shows a dispersion of typically a few tenths of an eV and its shape is very sensitive to the atomic geometry. The second band, just below $E_F$, exhibits a much larger dispersion of ~1.5–2 eV. Whatever the atomic structure, it disperses downwards when moving off $\bar{\Gamma}$ and has bonding character at $\bar{M}$ or $\bar{K}$. This band shows a more or less pronounced shoulder near $\bar{\Gamma}$, de-

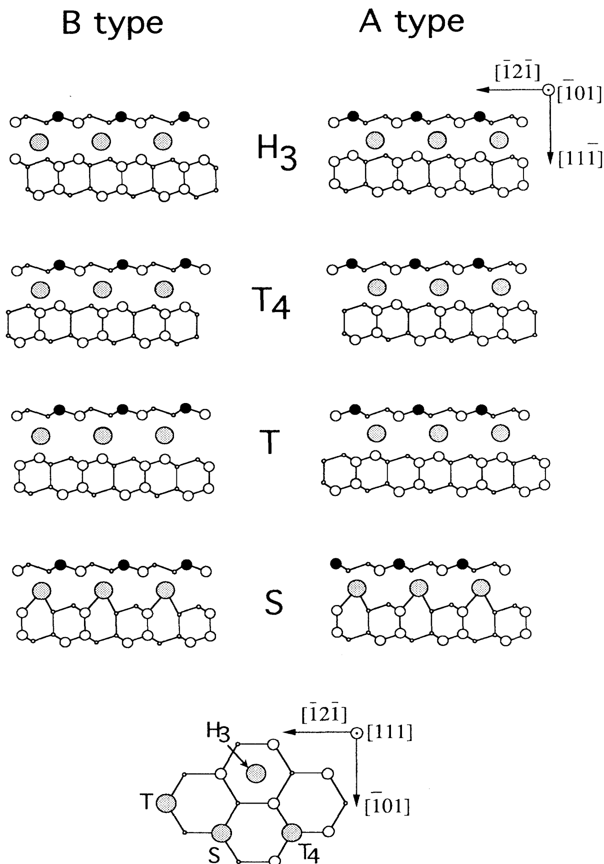


FIG. 3. Sketch of the eight typical interfacial structures tested in the calculations. The structure is projected along the [$\bar{1}01$] direction as in Fig. 1. The Er may sit in $T$ (top), $S$ (substitutional) $H_3$, and $T_4$ sites of the substrate and there are two possible orientations ( $A$ and $B$) of the topmost Si double layer. A top view of the $T$, $S$, $H_3$, and $T_4$ sites on Si(111) is also shown.

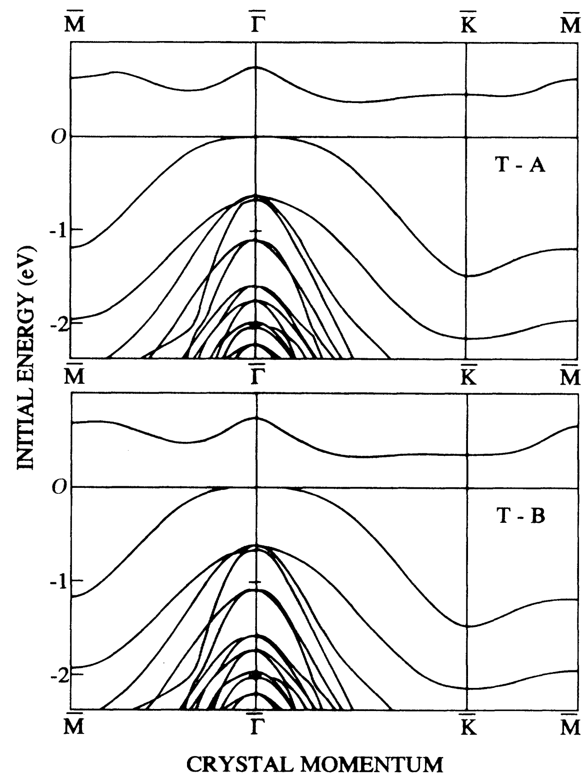


FIG. 4. Calculated bands for the *T-A* and *T-B* geometries along the symmetry lines of the surface Brillouin zone and for binding energies lower than ~2 eV. The values of the structural parameters are $d_{\rm up}=2.7$ Å, $d_{\rm down}=2.0$ Å, and $d^s_{\rm up}=3.0$ Å. Bulk geometry is adopted for the Si substrate layers. The energy scale is referred to the highest occupied energy level and corresponds to the Fermi energy $E_F$ when the silicide is predicted to be a metal.

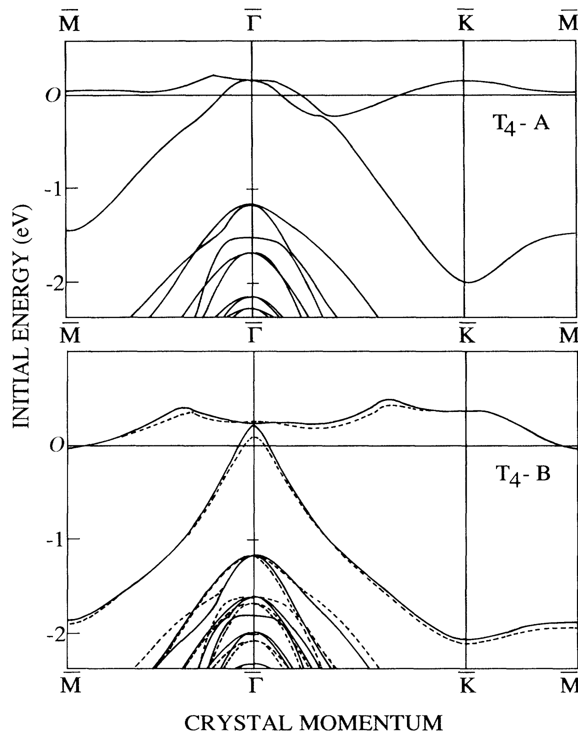


FIG. 5. Same as Fig. 4 but for $T_4$-$A$ and $T_4$-$B$ geometries and $d^s_{up}=2.0$ Å. The dashed curves ($T_4$-$B$ geometry) are for relaxed Si top double layer with $d_{up}=2.7$ Å, $d_{down}=1.8$ Å, and $d^s_{up}=2.0$ Å (top-layer structure of Ref. 9).

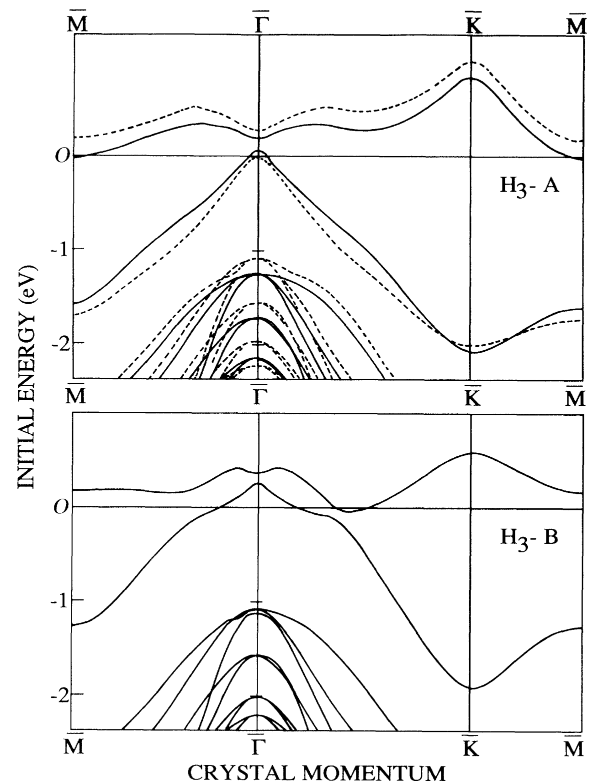


FIG. 6. Same as Fig. 4 but for $H_3$-$A$ and $H_3$-$B$ geometries and $d^s_{up}=2.0$ Å. The dashed curves ($H_3$-$A$ geometry) are for relaxed Si top double layer with $d_{up}=2.7$ Å, $d_{down}=1.8$ Å, and $d^s_{up}=2.0$ Å (top-layer structure of Ref. 9).

pending on atomic geometry, but its shape, location, and overall dispersion are in qualitative agreement with the prominent band observed experimentally in the 1–1.7-eV BE range. In contrast, the shape of the upper band is not consistent with the experimental data for four out of the six relevant models. Only the $H_3$-$A$ and $T_4$-$B$ geometries display the very characteristic minimum observed experimentally at $\bar{M}$. For the other geometries the band has a broad minimum at a general $k_{\parallel}$ point along $\bar{\Gamma}\bar{K}$ or $\bar{\Gamma}\bar{M}$. Actually, for the geometries with the Er in top sites, the calculations predict a substantial gap of about 0.4 eV, i.e., a semiconducting silicide layer. Thus, it appears that the topology of the calculated bands clearly favors two specific atomic geometries, namely $H_3$-$A$ and $T_4$-$B$. In these cases, the bands as well as the 2D Fermi surface are fairly well reproduced. There is a small overlap resulting in a nearly filled and a nearly empty band, with the related hole and electron pockets at $\bar{\Gamma}$ and $\bar{M}$, respectively. Thus, for these particular geometries the theory indeed predicts that the silicide is a 2D semimetal, in agreement with experiment.

Considering now the models with the Er in substitutional sites, namely $S$-$A$ and $S$-$B$, it is apparent that they can be safely ruled out on the basis of the calculated bands. Indeed, one obtains three as opposed to two bands crossing the Fermi level, and the Fermi surface, which consists of three branches, is now typical of a metal rather than a semimetal. This is in strong disagreement with experiment.

In the following discussion, we therefore concentrate on the $H_3$-$A$ and $T_4$-$B$ structures. We have tested the effect of a change in the structural parameters $d_{down}$, $d_{up}$, $d^s_{up}$, $d^s_{down}$ on the calculated bands. In a first calculation, the buckling of the Si top layer has been suppressed, i.e., a structure similar to bulk $ErSi_2$ has been adopted by setting $d_{up}=d_{down}=2.0$ Å, with the other parameters unchanged. The result is shown in Fig. 8 for the $T_4$-$B$ interfacial geometry. It is apparent that the upper band is modified in a drastic way. The minimum is now located along $\bar{\Gamma}\bar{K}$ as opposed to $\bar{M}$, where a strong antibonding character is observed instead. This is clearly incompatible with experiment and lends further support to the buckled Si top layer model. In a second test, the value $d_{down}$ has been reduced to 1.8 Å, the other parameters remaining unchanged. This corresponds to a contraction of the Er-Si interlayer spacing as well as an enhanced buckling of 0.9 Å of the Si top layer. The relevant parameters are those inferred from a comparison of recent Auger electron diffraction measurements with single scattering simulations.[9] As discussed in Ref. 9, these parameters imply an Er-Si bond-length contraction with respect to bulk $ErSi_{1.7}$, that can be related to a decrease in the number of nearest Si neighbors of the Er due to the buckling of the Si top layer. On the other hand, the enhanced buckling with respect to bulk Si is consistent with a charge transfer from Er to Si in the top layer.[15] The relevant bands for the $H_3$-$A$ and $T_4$-$B$ geometries

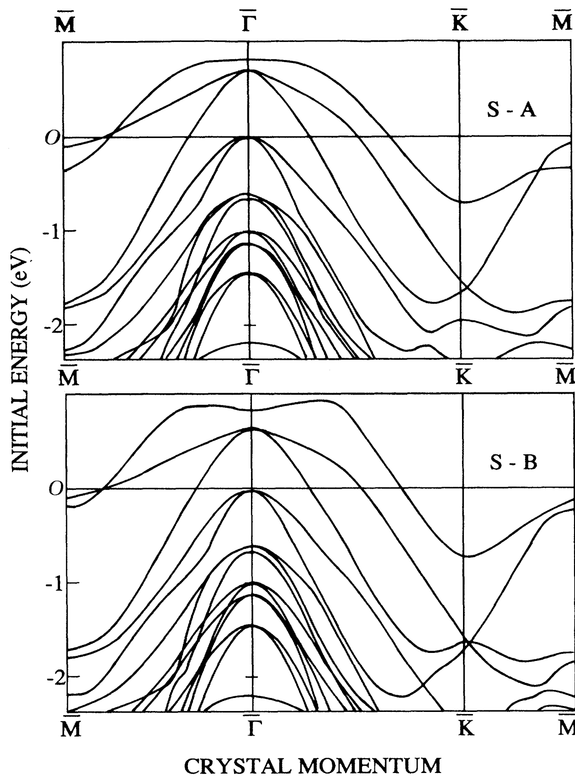


FIG. 7. Same as Fig. 4 but for $S$-$A$ and $S$-$B$ geometries and $d^s_{\rm down}=2.0$ Å.

are plotted in Figs. 5 and 6 as dashed lines. It can be seen that this relaxation of the Si top layer does not result in major changes in the general shape of the $E(k_\parallel)$ band dispersions. The main effect is a small shift of the bands, but none of the above structural conclusions is affected by these modifications. Yet, in the present system (experimentally a semimetal), the 2D Fermi surface is very sensitive and it can be seen that a small gap is now predicted for $H_3$-$A$. In contrast, in the $T_4$-$B$ geometry, the Fermi surface still exists and is fairly well reproduced as the size of the hole and electron pockets. We also find that the $T_4$-$B$ model has the lowest total electronic energy. These observations would favor the $T_4$-$B$ model. However, it is clear that the approximate character of the Hückel method implies that one cannot safely discriminate between $H_3$-$A$ and $T_4$-$B$ geometries on the basis of the present calculations only. Yet, since in recent experimental work[9] it has been shown that the buckled Si top layer adopts an orientation of type $B$, we are led to the conclusion that the interfacial geometry is most likely $T_4$-$B$.

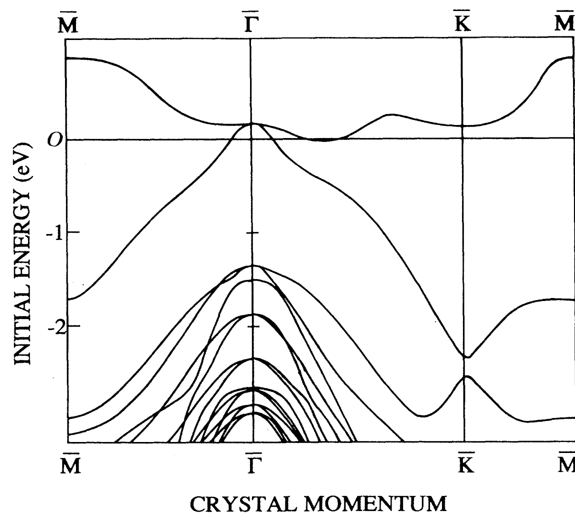


FIG. 8. Same as Fig. 4 but for $T_4$-$B$ interfacial structure and no buckling of the Si top layer, i.e., $d_{\rm up}=d_{\rm down}=d^s_{\rm up}=2.0$ Å. This structure corresponds to a single Er silicide layer with a bulklike geometry.

It is interesting to note here that the $T_4$-$B$ ($T_4$-$A$) and $H_3$-$A$ ($H_3$-$B$) geometries are in fact very similar. In both structures, the Er has six nearest Si neighbors forming two triangles with opposite (same) orientations, one of them just above and the other just below the Er layer. This explains the similarities observed in their respective band dispersions. There is, however, an additional Si neighbor at a similar distance just below the Er for the $T_4$ site. Possibly this sevenfold coordination might explain the higher stability of the $T_4$ geometry. Yet it is apparent that the orientation of the buckled Si top layer with respect to the substrate plays a major role, since the $T_4$-$A$ and $H_3$-$B$ geometries having the same coordination numbers as $T_4$-$B$ and $H_3$-$A$, respectively, result in band dispersions incompatible with experiment. To decide from a theoretical point of view which model has the lowest energy needs more sophisticated computations, for instance total-energy *ab initio* calculations, where the relaxation of the substrate has to be taken into account.[15] For the $T_4$-$B$ geometry, we have investigated the effect on the bands of a relaxation of the first Si substrate double layer by varying $d^s_{\rm up}$ and $d^s_{\rm down}$, thus allowing for a repulsion of 0.2 Å between the Er and the second Si layer. One observes (data not shown) a small change ($\leq 0.2$ eV) in the calculated band widths, but the overall shape and location of the bands with respect to $E_F$ remain unchanged. In particular, the experimental 2D Fermi surface is still well reproduced.

In Fig. 9, we directly compare experimental and calculated bands for the structural model $T_4$-$B$ with the buckled Si top layer structure of Ref. 9 and unrelaxed substrate. The agreement is qualitatively good even for the bands at binding energies larger than 2 eV. Generally, the experimental bands show less dispersion and are located at lower binding energies than the calculated ones. Similar discrepancies are observed in many instances, even with *ab initio* band calculations, and are partly related to the fact that photoemission measures excited states of the system. Because of the rather large number of substrate Si layers included in the slab, the calculations show numerous bands at higher binding energies that reflect the Si bulk continuum as shown by the expansion of the band states, in terms of atomic orbitals. For the sake of clarity, we do not show all these bands in Fig. 9, but present them in Fig. 10. These bands provide a fairly good simulation of the projected bulk band continuum on the SBZ and indicate that the upper almost-filled band

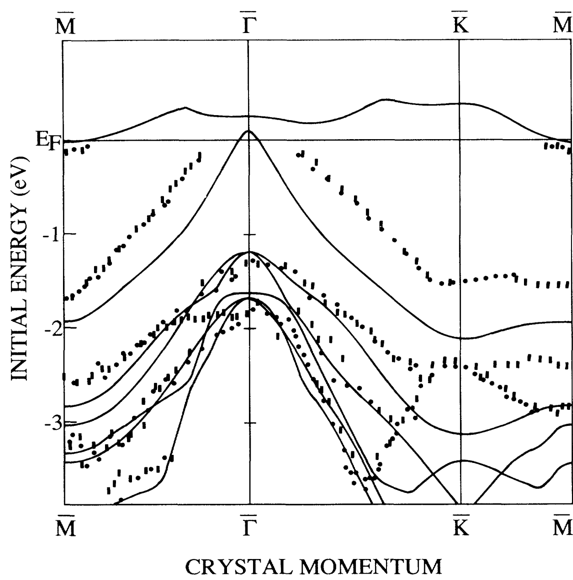


FIG. 9. Comparison of the calculated (full lines) and experimental bands along $\overline{\Gamma}\overline{M}$, $\overline{\Gamma}\overline{K}$, and $\overline{K}\overline{M}$. The structure adopted is $T_4$-$B$ with $d_{up}=2.7$ Å, $d_{down}=1.8$ Å, and $d_{up}^{s}=2.0$ Å. Bulk geometry is adopted for the Si substrate layers.

corresponds to true surface states localized in the silicide over the whole SBZ. This is in line with the very narrow and sharp features reflecting this band in the angle-resolved photoemission spectra,[8] as well as with the orbital analysis of the relevant wave functions. The upper almost-empty band exhibits over the whole SBZ strong hybridization between Er $5d$ and Si $3p$ states from the Si double layer just above and just below the Er. The almost-filled band has a similar character at $\overline{\Gamma}$, where the state mainly contains Er $5d_{z^2}$ and Si $3p_z$. Off $\overline{\Gamma}$, the band acquires progressively dominant Si $3p_z$ character and is markedly localized in the topmost Si double layer, i.e., it reflects the Si dangling bonds. This dangling-bond-derived band is essentially filled because of hybridization with Er $5d$, stabilization, and electron donation, and closely resembles the relevant band observed in As-terminated Si(111).[16] This contrasts with the half-filled dangling-bond band predicted for the ideal unstable Si(111) surface,[17,18] but the shape and overall dispersion are very similar. As expected, the band states observed at higher binding energies show generally a smaller hybridization with Er $5d$ and correspond essentially to bulk Si bands modified in the surface region by interaction with the energetically degenerate Er $5d$-Si $3p$ bonding states of the silicide layer. They exhibit generally the characteristic antibonding character of Si $3p$-derived bands at $\overline{\Gamma}$. Some bands show strong surface resonances in the silicide layer, which gives them a marked 2D character in photoemission. A typical example is the band observed at 1.3 eV at $\overline{\Gamma}$ and dispersing downwards in the 1.3–2.5-eV BE range.

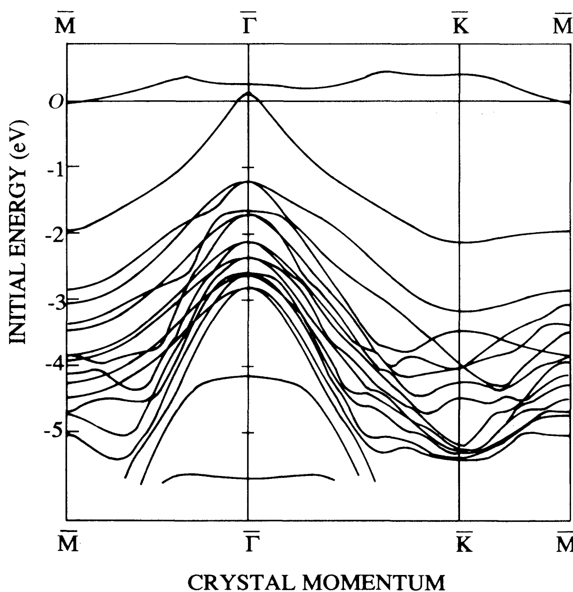


FIG. 10. Calculated bands for the $T_4$-$B$ geometry showing the deeper bands that simulate the Si bulk band continuum.

The present study suggests the following picture for the chemical bonding in the surface silicide. Among the three valence electrons of Er in the hexagonal layer, one of them is involved in the bonds to the Si double layer underneath which, in the absence of the layer, exhibits (upwards pointing) dangling bonds of an ideal Si(111) surface. In the presence of the silicide, the latter are saturated, and a closed-shell structure is obtained for the Si at the interface. Similarly, a second Er valence electron binds the Er layer to the top Si double layer and saturates the relevant (downward pointing) dangling bonds. Again this results in a closed-shell structure for the Si in the Si(111) plane just above the Er. Finally, because of the electropositivity of Er, the third Er valence electron fills to a large extent the band derived from dangling bonds of the topmost Si plane. This is equivalent to a double occupation for the outwards pointing dangling bonds of the Si top layer and establishes a particularly stable situation with closed-shell structure for all Si atoms. The relevant surface is quite inert, as is As-terminated Si(111). However, in the present case, because of screening and, in turn, approximate local charge neutrality, the actual charge transfer to the topmost Si must be much smaller than one. High-resolution Si $2p$ core-level measurements indicate charge transfers of a few tenths of an electronic charge.[19]

The above picture readily explains why the models with Er in substitutional sites ($S$-$A$ and $S$-$B$) result in calculated bands very different from the experimental ones and appear to be completely inadequate. Indeed, in this case, each Er has to saturate three as opposed to one dangling bonds per Si atom in the layer underneath. This needs already all available Er valence electrons. As a result, no electrons are left to bind the Er to the top Si double layer and to stabilize the upwards pointing dangling bonds. This results in an unoccupied dangling-bond band and explains the drastic changes in the topology of the calculated bands near $E_F$. In contrast, it is clear that all other models tested based on $T$, $T_4$, and $H_3$ sites satisfy the above electron-counting requirements and all of them

show an almost-occupied dangling-bond band. From a physical point of view, it is also not surprising that the calculations favor the high-coordination $H_3$ and $T_4$ configurations. The physical origin of the strong dependence of the calculated bands on the relative orientations of top and substrate Si double layers is less clear. This dependence constitutes an important result of the present study, in agreement with experiment, which shows that a definite orientation of the top Si double layer is indeed preferred.

## IV. CONCLUSION

We have compared the experimental and theoretical band structures of a 2D silicide epitaxially grown on Si(111). The computational method is the crystalline extension of the extended Hückel method. A series of reasonable structural models have been tested. The results show that the experimental bands can be well reproduced for two specific atomic models. In principle, the calculations are not very accurate, but more sophisticated band calculations are not likely to change substantially the overall topology of the bands. In this respect, the main weakness of the present calculations is that they do not take into account surface charge rearrangements and, in turn, the perturbation of the potential that results in a shift of the atomic levels. We have found that for reasonable shifts (of typically $\sim 0.5$ eV, as expected from charge transfers) of the diagonal elements $H_{ii}$, the bands shift on an absolute scale but their topology and location with respect to $E_F$ remains essentially unaffected. Since qualitative arguments related to the shape of the bands are used in the comparison between theory and experiment, this means that none of the structural conclusions drawn in the above discussion would be modified, and a series of possible models can be ruled out with a good degree of confidence. Along with recent experimental information on the orientation of the buckled Si top layer, our study strongly favors an interfacial geometry with the Er in $T_4$ sites and the top Si double layer rotated 180° around the surface normal with respect to the substrate layers. Thus, with a modest computational effort, one may obtain valuable structural information in favorable cases. From a quantitative point of view, the agreement between measured and calculated bands for the $T_4$-$B$ model is satisfactory and in line with the expected accuracy of the EHT method. The orbital origin of the prominent surface bands observed experimentally could be elucidated and a good physical picture of the electronic structure of this remarkable 2D silicide obtained. The present structural model should provide a good starting point for more refined calculations.

## ACKNOWLEDGMENTS

The computations have been performed at CCSC (Centre de Calcul du CNRS de Strasbourg) within the project "Calcul Numérique Intensif." The Laboratoire de Physique et de Spectroscopie Electronique is "Unité Associée au Centre National de la Recherche Scientifique No. 1435."

[1]N. Cherief, R. Cinti, M. de Crescenzi, J. Derrien, T. A. Nguyen Tan, and J. Veuillen, Appl. Surf. Sci. **41/42**, 241 (1989), and references therein.

[2]H. van Känel, R. Stalder, H. Sirringhaus, N. Onda, and J. Henz, Appl. Surf. Sci. **43**, 196 (1991), and references therein.

[3]K. N. Tu, R. D. Thompson, and B. Y. Tsaur, Appl. Phys. Lett. **38**, 626 (1981).

[4]J. Y. Duboz, P. A. Badoz, A. Perio, J. C. Oberlin, F. Arnaud d'Avitaya, Y. Campidelli, and J. A. Chroboczek, Appl. Surf. Sci. **38**, 171 (1989).

[5]J. A. Knapp and S. T. Picraux, Appl. Phys. Lett. **48**, 466 (1986).

[6]F. Arnaud d'Avitaya, A. Perio, J. C. Oberlin, Y. Campidelli, and J. A. Chroboczek, Appl. Phys. Lett. **54**, 2198 (1989).

[7]P. Paki, U. Kafader, P. Wetzel, C. Pirri, J. C. Peruchetti, D. Bolmont, and G. Gewinner, Phys. Rev. B **45**, 8490 (1992).

[8]P. Wetzel, C. Pirri, P. Paki, J. C. Peruchetti, D. Bolmont, and G. Gewinner, Solid State Commun. **82**, 235 (1992).

[9]P. Wetzel, C. Pirri, P. Paki, D. Bolmont, and G. Gewinner, Phys. Rev. B **47**, 3677 (1993).

[10]R. Hoffmann, J. Chem. Phys. **39**, 1399 (1963).

[11]M. H. Wangbo and R. Hoffmann, J. Am. Chem. Soc. **100**, 6093 (1978).

[12]J. H. Ammeter, H. B. Brügi, J. Thibeault, and R. Hoffmann, J. Am. Chem. Soc. **100**, 3686 (1976).

[13]C. Minot, M. A. Van Hove, and G. A. Somarjai, Surf. Sci. **127**, 441 (1983).

[14]R. Hoffmann and P. Hoffmann, J. Am. Chem. Soc. **98**, 598 (1976).

[15]See, for instance, M. Lannoo and P. Friedel, in *Atomic and Electronic Structure of Surfaces—Theoretical Foundations* (Springer, Berlin, 1991).

[16]M. S. Hybertsen and S. G. Louie, Phys. Rev. B **38**, 4033 (1988).

[17]K. C. Pandey and J. C. Phillips, Solid State Commun. **14**, 439 (1974); Phys. Rev. Lett. **32**, 1433 (1974).

[18]K. Hirabayshi, J. Phys. Soc. Jpn. **27**, 1475 (1969).

[19]P. Wetzel, C. Pirri, D. Bolmont, and G. Gewinner (unpublished).